

Estimating labile particulate iron concentrations in coastal waters from remote sensing data

Anna R. McGaraghan¹ and Raphael M. Kudela¹

Received 22 January 2011; revised 21 November 2011; accepted 25 November 2011; published 1 February 2012.

[1] Owing to the difficulties inherent in measuring trace metals and the importance of iron as a limiting nutrient for biological systems, the ability to monitor particulate iron concentration remotely is desirable. This study examines the relationship between labile particulate iron, described here as weak acid leachable particulate iron or total dissolvable iron, and easily obtained bio-optical measurements. We develop a bio-optical proxy that can be used to estimate large-scale patterns of labile iron concentrations in surface waters, and we extend this by including other environmental variables in a multiple linear regression statistical model. By utilizing a ratio of optical backscatter and fluorescence obtained by satellite, we identify patterns in iron concentrations confirmed by traditional shipboard sampling. This basic relationship is improved with the addition of other environmental parameters in the statistical linear regression model. The optical proxy detects known temporal and spatial trends in average surface iron concentrations in Monterey Bay. The proxy is robust in that similar performance was obtained using two independent particulate iron data sets, but it exhibits weaker correlations than the full statistical model. This proxy will be a valuable tool for oceanographers seeking to monitor iron concentrations in coastal regions and allows for better understanding of the variability of labile particulate iron in surface waters to complement direct measurement of leachable particulate or total dissolvable iron.

Citation: McGaraghan, A. R., and R. M. Kudela (2012), Estimating labile particulate iron concentrations in coastal waters from remote sensing data, *J. Geophys. Res.*, 117, C02004, doi:10.1029/2011JC006977.

1. Background

[2] Numerous studies have been conducted to better understand the distribution and variability of iron in coastal upwelling regions. Iron can be a limiting factor governing phytoplankton growth in large regions of the ocean, particularly in high-nutrient, low-chlorophyll (HNLC) regions [cf. Boyd *et al.*, 2007]. Despite the presence of fluvial and continental shelf sources of iron, coastal upwelling environments can also at times be iron limited [Bruland *et al.*, 2001, 2005; Hutchins *et al.*, 1998, 2002; Johnson *et al.*, 1999]. Indeed, it has been suggested that the large-scale poleward trend in phytoplankton biomass and higher trophic level productivity along the U. S. west coast is due to the relative availability of iron [Chase *et al.*, 2007; Ware and Thomson, 2005]. Our ability to accurately estimate iron concentrations is a critical step in understanding the distributions and abundance of phytoplankton, which in turn are the basis for higher trophic level biology, carbon sequestration, and many other indicators of ocean health. For example, harmful blooms of the toxigenic diatom *Pseudo-nitzschia* has been directly linked to iron

availability in California coastal waters and elsewhere [Rue and Bruland, 2001; Wells *et al.*, 2005].

[3] Monterey Bay, California, an active upwelling region, has been described as a “mosaic” of iron-replete and iron-deplete conditions [Hutchins and Bruland, 1998]. Reevaluation of the iron requirements for coastal phytoplankton, particularly diatoms, suggests that iron depletion and limitation may be more commonly observed than would be assumed based solely on proximity to the continental shelf [Bruland *et al.*, 2001]. While iron has been routinely measured in ocean environments for many years, developing a system by which iron-replete and iron-deplete conditions in dynamic coastal regions can be identified and monitored over time presents a challenge to oceanographers. The Monterey Bay Aquarium Research Institute (MBARI) and the Center for Integrated Marine Technology (CIMT) have in combination collected over ten years (1998–2008) of time series data, including iron, from Monterey Bay, providing a unique opportunity to assess the seasonal and interannual variability of iron and its associated impacts on the phytoplankton community.

[4] A variety of methods for the determination of iron in seawater exist, and are frequently modified and adapted [Johnson *et al.*, 2007]. Most are time and labor intensive and are not necessarily amenable to extrapolation for larger spatial and temporal scales. Owing to the highly variable nature of the iron supply in coastal areas and the great importance of iron to biological productivity, a need exists for a convenient and consistent way to estimate iron concentrations remotely.

¹Department of Ocean Sciences, University of California, Santa Cruz, California, USA.

Bio-optics can provide a critical linkage between parameters that are easily and nonintrusively measured and the many biological and chemical parameters that we desire to measure rapidly, but which are not conducive to high spatial or temporal observations (e.g., iron).

[5] Ocean color satellites have frequently been used to track surface plumes, particularly storm water and river plumes, by taking advantage of changes in color (particularly colored dissolved organic material (CDOM) absorption) and particle backscatter [Nezlin *et al.*, 2008; Warrick *et al.*, 2007]. Given sufficient ground-truth data, it is also possible to correlate bulk bio-optical properties to covarying biogeochemical parameters such as salinity for which there is no direct optical estimate [Palacios *et al.*, 2009]. As the light-scattering properties of a particle depend on its chemical composition, index of refraction, size, and shape, Twardowski *et al.* [2001] and Boss *et al.* [2004] have shown that bulk particle composition can be determined via data collected with optical measurements. Building on this basic information, Kudela *et al.* [2006] identified the ratio of backscatter to fluorescence as a proxy for the concentration of acetic acid leachable iron in the water column [see Kudela *et al.*, 2006, Figure 12], and Benoit *et al.* [2010] demonstrated that for particle-dominated water bodies such as San Francisco Bay, there is a direct correlation between metal concentration and suspended particulate matter. Kudela *et al.* [2006] argued that acid leachable iron was a good indicator of bio-available iron in coastal waters, since the leachable fraction acts as a reservoir for the biologically labile dissolved fraction; Elrod *et al.* [2008] similarly showed a highly significant linear relationship between dissolvable iron and dissolved iron for Monterey Bay, while Fitzwater *et al.* [2003] discuss the importance of the particulate iron pool as a “biologically available” fraction. The dissolved iron fraction is in turn controlled by strong and weak iron-binding ligands, making the concentration of dissolved iron relatively invariant while the particulate fraction can vary by orders of magnitude [Buck *et al.*, 2007; Elrod *et al.*, 2008; Kudela *et al.*, 2006].

[6] Kudela *et al.* [2006] collected in situ fluorescence and backscatter data using a HobiLabs HS-6 for comparison to matched acid leachable (particulate) iron samples in the coastal waters near Point Reyes, CA. Here we develop a remote sensing proxy for labile particulate iron that also uses backscatter and fluorescence. Our primary goal is to demonstrate that this bio-optical proxy, in conjunction with a statistical model incorporating other environmental parameters, is reasonably robust at estimating labile particulate iron in surface waters of the Monterey Bay region. We then describe the spatial and temporal patterns observed from this time series. This proxy is not intended to replace traditional iron sampling methods, but rather provides oceanographers with an additional tool for estimating iron concentrations when shipboard and laboratory sampling are not available. A more detailed description of the biogeochemistry of iron in the Monterey Bay region is given by Elrod *et al.* [2008, and references therein].

2. Data and Methods

2.1. Center for Integrated Marine Technology

[7] The Center for Integrated Marine Technology (CIMT) was a collaborative effort between several institutions that

conducted monthly sampling between 2002 and 2007. The cruises focused on the Monterey Bay region of the Monterey Bay National Marine Sanctuary, from Point Lobos to Point Año Nuevo ($\sim 36.5^\circ$ to 37.1° N), extending west to $\sim 122.1^\circ$ W (Figure 1). At each station, a Seabird SBE-19 collected conductivity (salinity), temperature, and depth measurements during vertical profiles to 200 m or to within about 10 m of the bottom at shallow-water stations. Salinity and temperature data were averaged over the top 5 m to correspond with trace-metal sampling; this was within the surface mixed layer for all stations. From 2002 to 2005, water samples were collected using Niskin bottles (retrofitted with silicon bands) affixed directly to the hydrowire. During 2006–2007, the SBE-19 was integrated with a 12-bottle rosette system with the same bottle configuration. Discrete water samples were collected at 5 m at all stations, and at 0, 10, and 25 m for stations T401 (near the M1 mooring) and T101 (northern bay; see Figure 1). Total chlorophyll was determined using the nonacidification technique [Welschmeyer, 1994]. Separate samples were filtered on Poretics polycarbonate membranes for size-fractionated chlorophyll (size fractions varied through the duration of the program, and included 5, 10, and 20 μm filters).

[8] For trace metal measurements, seawater was collected with a trace metal clean “fish” pumping system into pre-cleaned 2 L bottles at each station. Samples were stored cold for the duration of the cruise, and brought back to the lab for processing. Water samples were filtered on 10 μm and 0.4 μm Nuclepore polycarbonate membrane filters and frozen. For iron analysis, filters were leached for 2 h in 25% (4.5 M) acetic acid [Landing and Bruland, 1987]. Analysis for acid leachable iron was as described by Landing and Bruland [1987], with final concentrations determined by inductively coupled plasma-sector field mass spectrometry (ICP-SFMS) following the method of Hurst and Bruland [2008]. Reported analytical precision was 10% for CIMT samples. We refer to these measurements as acid leachable iron, or HacFe. At the same stations, a vertical profile was collected using a HOBI-Labs HS-2 backscatter/fluorometer (443 and 671 nm), referred to as b_{b}/fl to distinguish it from the satellite-derived b_{b}/FLH .

2.2. MBARI Time Series

[9] Two oceanographic stations maintained by MBARI were used for this study, C1 and M1. C1 is located at 36.797°N , 121.847°W , 5 km offshore of Moss Landing, California (Figure 1). The M1 mooring is located 20 km from Moss Landing at 36.747°N , 122.022°W . MBARI also maintains a mooring at location M2 (36.70°N , 122.39°W) 45 km from shore, with corresponding in situ (shipboard) iron measurements. We examined data from this station, but did not focus on the M2 location for this study because of the low absolute values and dynamic range of iron concentrations and the likelihood that our models do not apply to offshore waters.

[10] From August 1998 to December 2005, MBARI conducted a sampling program at these stations that included both particulate and dissolved iron measurements (time series for these stations exist for 1989 to the present, but the remainder of the time series did not include iron). For our analysis, the MBARI dissolvable iron data set was used. Seawater was collected at a depth of 1–2 m with a Teflon

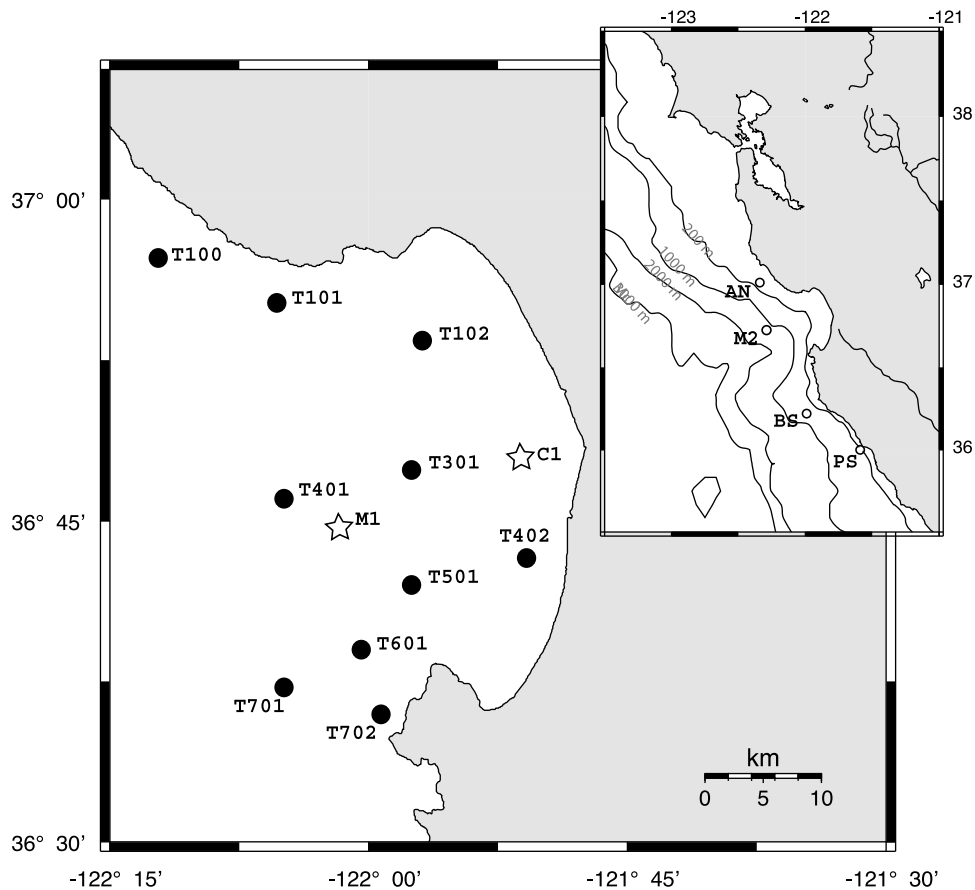


Figure 1. Monterey Bay, California, shown with time series station locations from the CIMT program (solid circles) and MBARI stations (open stars). Locations for MODIS b_{bp} /FLH data at Año Nuevo (AN), Point Sur (PS), and Big Sur (BS) are provided on the inset map.

pumping system and stored overnight at $<5^{\circ}\text{C}$ [Johnson *et al.*, 1999]. For dissolvable iron, samples were acidified to pH 3 using ultrapure acid, left for 1 min, and analyzed [Johnson *et al.*, 1999]. Flow injection analysis with chemiluminescence detection was used as described by Obata *et al.* [1993]. We refer to these measurements as “dissolvable iron,” DVBLFe, following the notation of Elrod *et al.* [2008]. Estimated coefficient of variation (CV) for these data was 2–10% (V. Elrod, personal communication, 2011). This variance is similar to both the CIMT data and previous reports for coastal California waters: we estimated the CV for an open ocean region with low iron concentrations [Johnson *et al.*, 2003] to be 18.18%, while analysis of short transects in Monterey Bay [Fitzwater *et al.*, 2003] provide ~ 2 –22% CV. Both of the latter estimates include analytical uncertainties and the inherent variability of the field data, which were collected using a pumped system while the vessel was underway, in contrast to the MBARI data set used herein, where the ship was on station during sample collection.

2.3. Satellite Measurements: MODIS Aqua

[11] Data from the Moderate Resolution Imaging Spectroradiometer (MODIS) Aqua sensor were used for this study. MODIS data were processed from Level 1A using SeaDAS software, applying calibrations for ocean remote sensing

developed by the MODIS Ocean Biology Processing Group. Processing followed standard NASA protocols for MODIS version R1, except that the high light and stray light masks were disabled. Level 2 data used for our bio-optical iron proxy included fluorescence line height (FLH) and 443 nm particulate backscatter (b_{bp}) using the QAA model [Lee *et al.*, 2002]. Resulting image data were mapped to a cylindrical projection; the true resolution of FLH, chlorophyll and SST images are at best ~ 1 km at nadir. After spatial projection, data were temporally averaged to 1 image/day to account for acquisition of multiple images within a few hours owing to overlapping satellite swaths; images were manually checked for quality, and images with poor coverage or obvious noise due to poor sensor angle were discarded ($<1\%$ of all images). A region of 0.05 degrees latitude and 0.08 degrees longitude, centered on the site of interest (e.g., station and mooring locations), was extracted corresponding to a 7×7 pixel region, or ~ 50 km². This spatial binning represents a compromise between higher resolution and fewer matchups. Data for matchups were also extracted at 1 km (1 pixel) resolution within ± 1 day of in situ observations, and for a 5 day window using the 7×7 spatial region. The pixel-level data were quality controlled by removing any FLH value greater than $1 \text{ mW cm}^{-2} \mu\text{m}^{-1} \text{ sr}^{-1}$, and any chlorophyll value greater than 65 mg m^{-3} . The remaining data were averaged using either a simple mean or median, ignoring zero

Table 1. Parameters Used in the Multiple Linear Regression Model^a

Variable (X_i)	Partial Correlation Coefficient	Weighting (X_j)	Suggested Response Factor
B1 (constant)		2.115	
B2 (constant)		4.310	
LOG(b _{bp} /FLH)	0.463	0.448	Particulate iron proxy
LOG(CHL)	0.238	0.186	Organic/inorganic particles
SST	-0.326	-0.256	Source water and season
Pajaro river flow	0.465	0.003	Source of iron
Salinas river flow	0.383		Source of iron
M1 upwelling index	0.121	0.006	Source water and season
PFEL upwelling index	0.106		Source water and season
Day length	-0.150		Seasonality

^aAll factors used in the model (“Weighting” column) were significant ($p < 0.05$). Variables not used were removed on the basis of Akaike Information Criteria scores and were typically highly covarying with an included parameter (e.g., Pajaro and Salinas river flow). SST, sea surface temperature.

values ($n = 99$ satellite versus in situ matchups for DVBLFE and $n = 123$ for HAcFe). For monthly, seasonal, and annual averages, satellite data points greater than 4 standard deviations from the mean were removed prior to averaging. The labile particulate iron (HAcFe and DVBLFE) were subsequently compared to MODIS (b_{bp}(443)/FLH) data. For convenience, units and wavelengths are omitted from this ratio for the remainder of the manuscript, and the ratio is referred to as b_{bp}/FLH. Subsequent analysis included derived chlorophyll, sea surface temperature, upwelling index, river flow, and day length.

2.4. Environmental Data

[12] River flow data for the Salinas and Pajaro were obtained from USGS gage stations 11159000 and 11125000, respectively, reported as cubic feet per second. Daily upwelling indices (UI) were obtained from two sources. The Pacific Fisheries Environmental Laboratory UI for 36°N, 122°W is based on a 3° pressure field calculated every 6 h. A second UI was determined using daily wind data from the MBARI M1 mooring by calculating daily Ekman transport as a function of hourly wind stress. Thus the PFEL UI provides a mesoscale estimate, while the M1 UI is a local (point source) estimate. Day length was calculated using a standard solar elevation model assuming a flat horizon.

2.5. Statistics

[13] A simple model was developed for the prediction of DVBLFE from b_{bp}/FLH and environmental parameters with multiple linear regression using Mstat 12 (SPSS). We considered $p < 0.05$ as significant for this project. For the statistical model, a backward stepwise linear regression was conducted using the Akaike Information Criteria (AIC) to identify the most robust set of parameters for inclusion. The dependent variable was DVBLFE, and the independent parameters are provided in Table 1. We applied a natural log transformation to DVBLFE, chlorophyll, and b_{bp}/FLH from MODIS and the C1 and M1 iron data to achieve normality in the data distributions prior to determination of the linear regression. A Shapiro-Wilk test was used to confirm normality, while a constant variance test was used to verify the appropriate application of the regression model. Additional

models were built using HAcFe and the combined data set following the same procedures. To differentiate between the bio-optical proxy and the regression models, we use “bio-optical proxy” to refer to the b_{bp}/FLH relationship, and “MLR model” to refer to the multiple linear regression models.

3. Results

3.1. CIMT and MBARI Time Series

[14] For this study, HAcFe values were averaged using either seasonal or annual time periods. For seasonal averages, we delineated the seasons as Oceanic (July, August, September, and October), Davidson (November, December, January, and February) and Upwelling (March, April, May, and June), as described by *Pennington and Chavez* [2000] and historically by *Skogsberg and Phelps* [1946]. When averaged annually, chlorophyll *a* and labile particulate iron did not follow the same trends; years with high average iron concentrations exhibited low average chlorophyll, and high-chlorophyll years exhibited low average iron. Spatially, iron concentrations varied between the northwestern part of Monterey Bay (CIMT stations T100, T101 and T102), and the southern region (T501, T601, and T701; Figure 1) with significantly higher (p value = 0.028) average annual HAcFe concentrations in the northern versus southern bay for all years. The annual averaged HAcFe concentrations for the entire domain showed a pattern of alternating relative high-iron and low-iron years, with 2003 being a high-iron year, 2004 low iron, etc. (Figure 2a).

[15] The MBARI time series data [*Elrod et al.*, 2008; *Johnson et al.*, 2001] are derived from three stations (C1, M1, M2) located at increasing distances from shore in Monterey Bay. DVBLFE at these three locations showed an onshore-offshore gradient in iron, with the highest iron concentrations nearshore [*Elrod et al.*, 2008; *Johnson et al.*, 2001]. For all sampling years, the annual averaged concentration of DVBLFE at C1 was significantly higher than at M1 (Figure 3a, p value = 0.031, paired t test). Annual averages for C1 exhibited temporal patterns similar to the CIMT data, with 2003 and 2005 being high-iron years relative to 2002 and 2004 (Figures 2 and 3).

3.2. Bio-optical Iron Proxy

[16] To determine whether b_{bp}/FLH from MODIS serves as a robust proxy for DVBLFE we matched each measurement of DVBLFE and HAcFe with the closest (temporally) available MODIS data point (Figure 4). The DVBLFE were also compared to coincident chlorophyll *a* measurements seasonally and for the entire data set by applying an ordinary least squares (OLS) regression. There was only a modest degree of correlation between DVBLFE and chlorophyll (Oceanic, Davidson, and Upwelling R^2 : 0.362, 0.000, and 0.002, respectively). The relationship between backscatter and labile particulate iron is improved by normalizing to FLH but not when normalizing to chlorophyll (Figure 4). To assess the sensitivity to matchup procedures, we also conducted the same analysis for b_{bp}/FLH using reduced spatial averaging (1 km pixels) and increased temporal binning (5 day averages). The reduced spatial averaging did not improve the correlation, but did result in greatly reduced matchups owing to missing satellite data. The increased

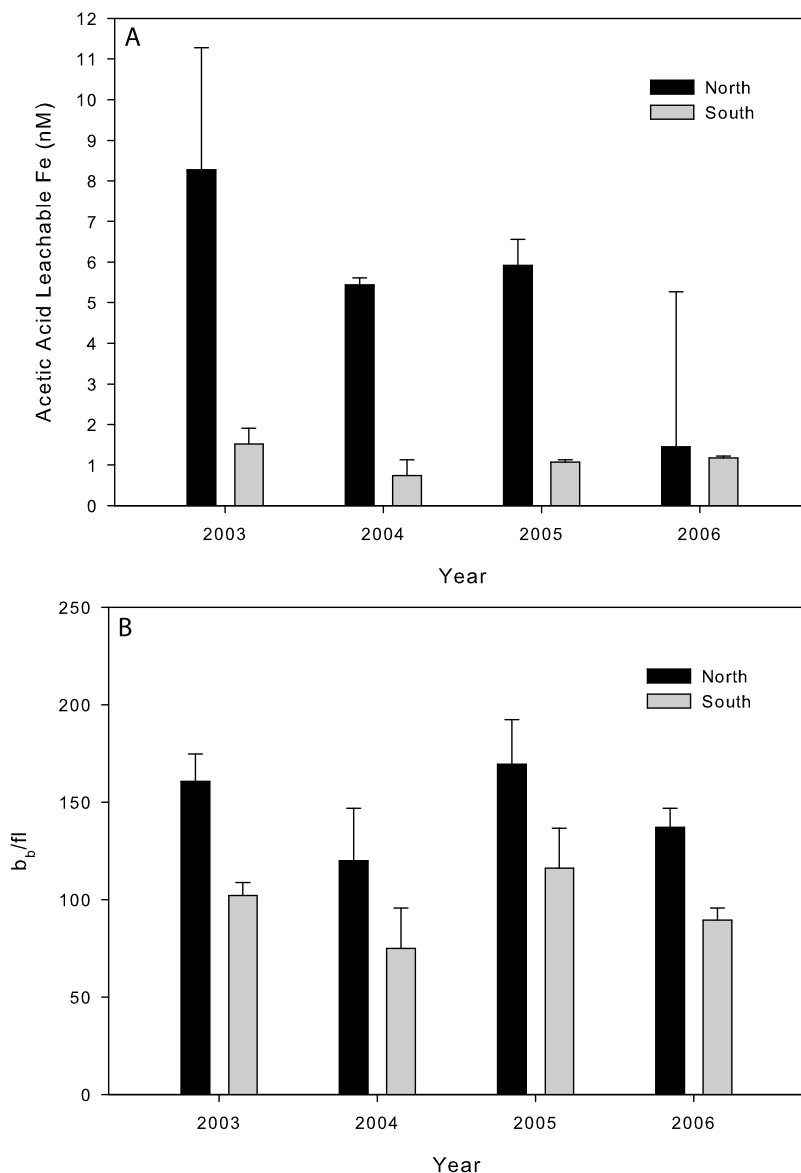


Figure 2. (a) HAcFe (nM) for 2003–2006 from northern CIMT stations (T100, T101, and T102; black bars) and southern CIMT stations (T501, T601, and T701; gray bars). (b) The b_b/f_l for 2003–2006 from northern and southern stations.

temporal binning resulted in statistically identical linear regressions between b_{bp}/FLH and labile particulate iron (ANCOVA), but with increased variability ($R = 0.341$ versus $R = 0.482$).

[17] On the basis of the good correspondence between b_{bp}/FLH and labile particulate iron, we used C1 and M1 data from the MODIS Aqua satellite to compare with DVBLFe. For all sampling years the average b_{bp}/FLH at C1 was significantly higher than at M1 (Figure 3b, p value = 0.004, paired t test), supporting the pattern identified from the in situ iron data. When divided seasonally into Oceanic, Davidson, and Upwelling periods (July–October, November–February, and March–June), MODIS optical data at C1 showed the same patterns as was detected by *Elrod et al.* [2008] with the b_{bp}/FLH ratio highest during the Davidson season and lowest during the Oceanic season. At the M1

mooring, the b_{bp}/FLH ratio was highest in the Davidson season in 2002, 2004, and 2005, and in the Upwelling season in 2003 and 2006. The DVBLFe at M1 was highest during the Upwelling season for all years [*Elrod et al.*, 2008].

[18] The direct correlations between DVBLFe and b_{bp}/FLH were 0.59, 0.59, and 0.13 for the Upwelling, Oceanic, and Davidson periods, respectively, considerably better than for chlorophyll but with a substantially weaker relationship during the autumn (Davidson) period. The correlations for C1 and M1 were similar (0.41 and 0.40) while the station by season correlations were in agreement with the combined data (0.54, 0.46, 0.41 for C1 and 0.53, 0.53, 0.09 for M1 during Upwelling, Oceanic, Davidson periods). The reduced correlation onshore (C1) and especially offshore (M1) during autumn suggests that the bio-optical proxy is weakest during this period when offshore waters tend to move shoreward

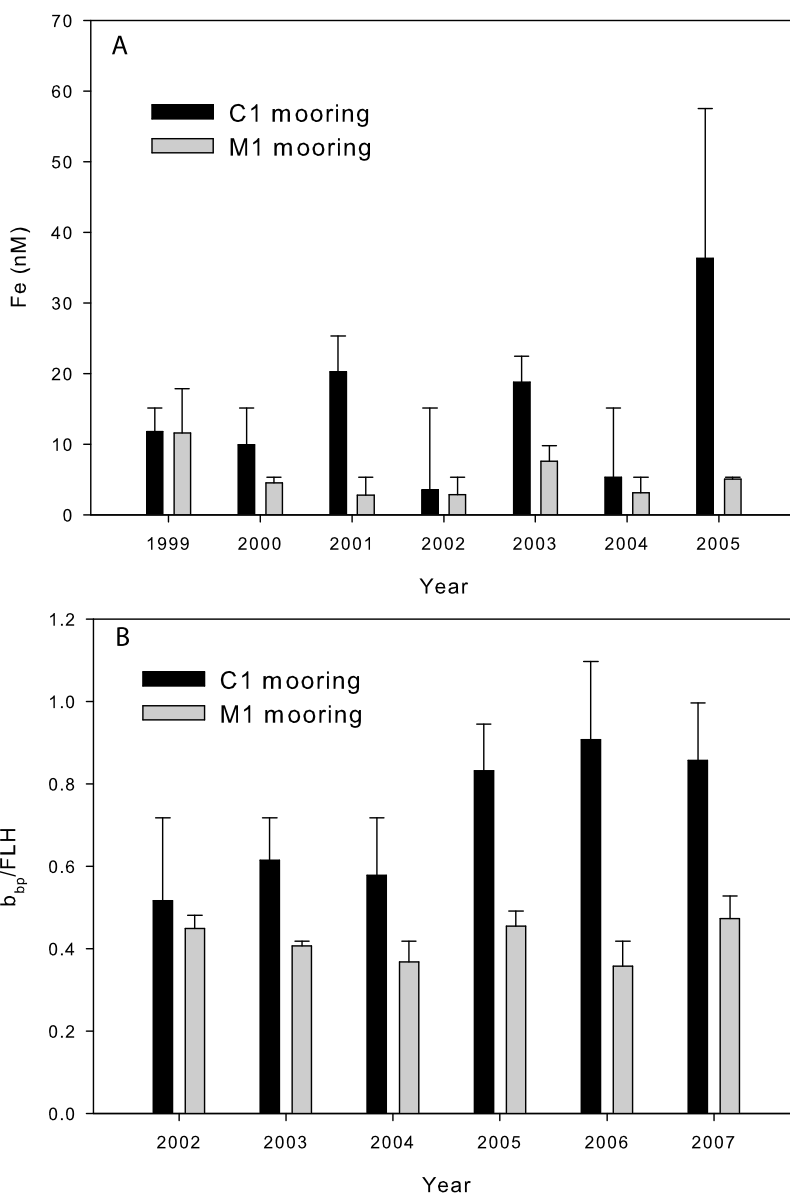


Figure 3. (a) DVBLFe (nM) from MBARI stations C1 and M1 for 1999–2005. (b) MODIS Aqua b_{bp}/FLH for C1 and M1 locations, 2002–2007.

and DVBLFe is at its seasonal low point [Pennington and Chavez, 2000; Johnson *et al.*, 2001], consistent with the observation that the data from M2 exhibited low variability in both optical properties and DVBLFe.

[19] Using the combined data set (C1 and M1, all seasons), we determined the error associated with the direct linear regression of DVBLFe and b_{bp}/FLH by estimating the root mean square error (RMSE) = 3.27 nM DVBLFe, or 93% error for the (log-transformed) linear regression. For comparison, the mean (\pm SD) DVBLFe was 11.2 (30.1) nM for the data used herein ($n = 99$), with coefficients of variation of 121% for C1 ($\bar{x} = 15.83 \pm 19.19$ nM, $n = 121$), 98% (4.93 ± 4.85 nM, $n = 110$) for M1, and 63% (1.29 ± 0.81 nM, $n = 100$) for M2, or 174% (7.35 ± 12.75 nM) for all data reported by Elrod *et al.* [2008].

3.3. Statistical Estimates of Labile Particulate Iron

[20] Building on the correspondence between b_{bp}/FLH and labile particulate iron, we added other environmental variables to generate a statistical predictive model. The parameters tested are provided in Table 1 and were applied to

$$\text{LOG}(\text{Fe}) = B1 * [B2 + \sum(\text{Xi} * \text{Xj})], \quad (1)$$

where LOG(Fe) is the natural log-transformed predicted DVBLFe (nM), B1 is a constant to adjust the linearity of the fit, B2 is a constant (intercept), and Xi, Xj are the weightings and environmental variables listed in Table 1. For this model, using all available data from C1 and M1 ($n = 99$), $R = 0.696$ ($R^2 = 0.484$) and root mean square error (RMSE) = 76.6%

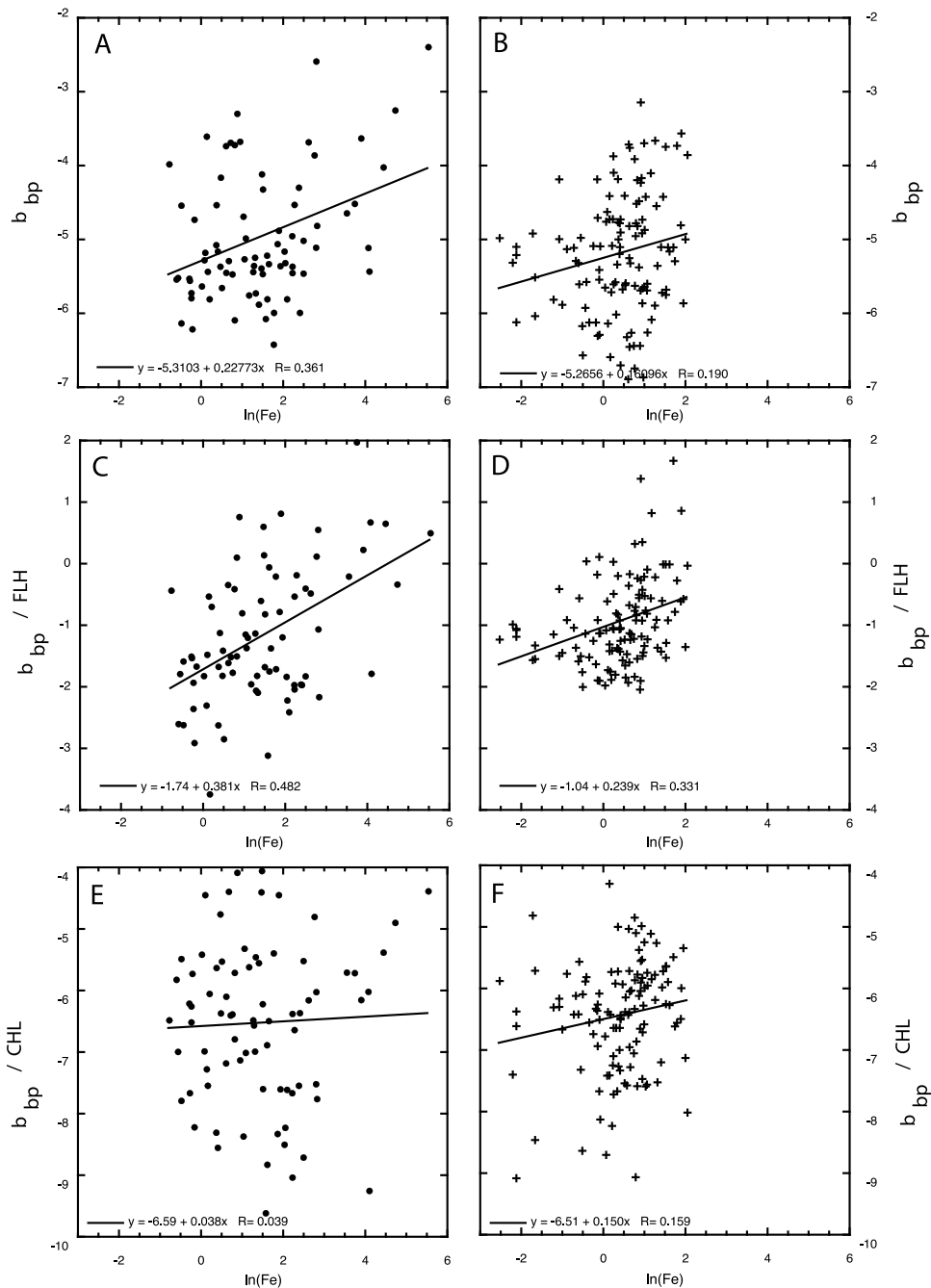


Figure 4. Satellite-derived b_{bp} plotted versus in situ (a) DVBLFe and (b) HACFe, with a best fit ordinary least squares regression (solid line and equation). The backscatter data are then normalized to (c, d) FLH and (e, f) chlorophyll. The b_{bp}/FLH relationship exhibits the best fit to the in situ iron measurements, as indicated by the higher R values.

(Figure 5). The predictive relationship is driven primarily by MODIS b_{bp}/FLH (Table 1) consistent with previous observations [Kudela *et al.*, 2006]. This model was applied to the CIMT HACFe data as an independent data set ($n = 123$). The fit was similar (Table 2), with $R = 0.596$ and $\text{RMSE} = 88.3\%$. A model was also built with the combined data set, with similar results ($R = 0.623$, $\text{RMSE} = 83.3\%$). All models identified the same subsets of environmental variables (based on AIC) with slightly different weighting functions. No

improvement was obtained by applying seasonal (Upwelling, Oceanic, and Davidson) models. We chose to use the MBARI model for two reasons. First, the MBARI time series has reduced spatial coverage but much better temporal coverage, resulting in a broader distribution of particulate iron data and associated environmental variables. Second, as discussed below, DVBLFe and HACFe are not the same estimates of particulate iron, and should be treated as independent estimates of a similar biogeochemical property.

Table 2. Model Results for Particulate Iron Using the Best Model Fit From the MBARI DVBLFe Data^a

Data Set	Data Points (n)	Slope (Intercept)	R (R ²)	RMSE (%)
MBARI	99	0.828 (0.509)	0.696 (0.484)	76.6
CIMT	123	1.270 (0.449)	0.596 (0.355)	88.3
Merged	222	0.833 (0.577)	0.623 (0.388)	83.3
Minus Chl	99	1.002 (1.57)	0.672 (0.451)	78.2

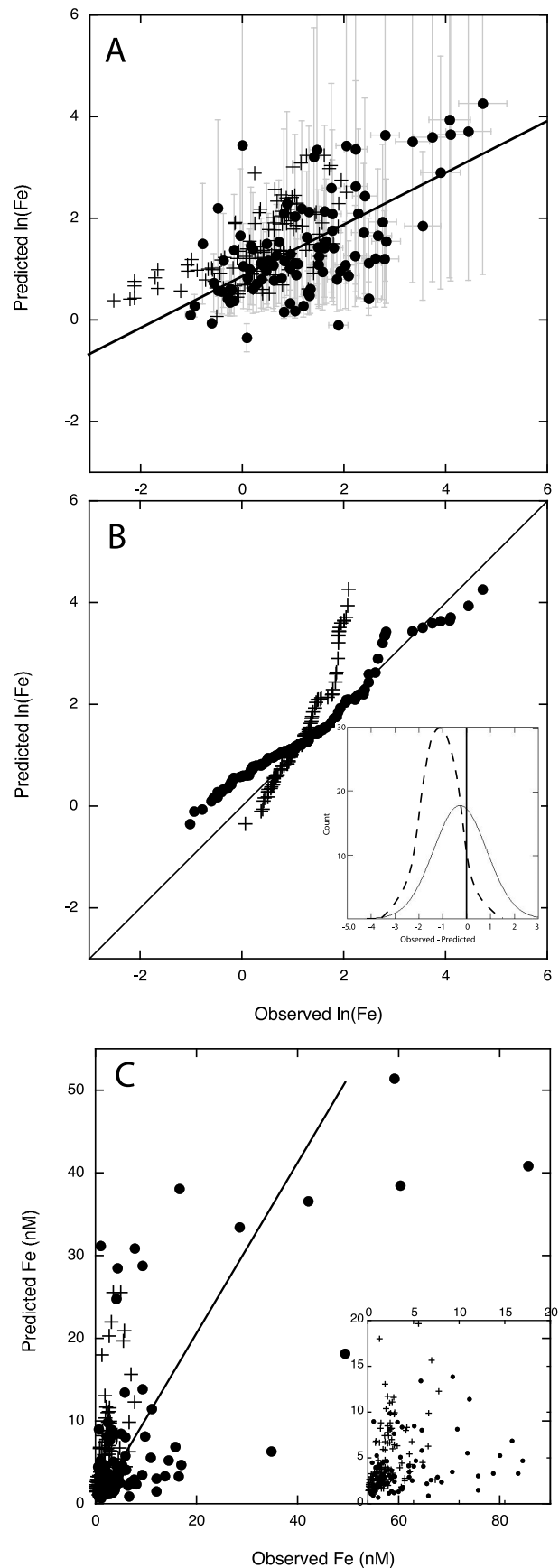
^aFor comparison, summary statistics are provided for the same model applied to the CIMT HAcFe data and to the merged (CIMT and MBARI) data. The “Minus Chl” row provides the fit for the MBARI model run with the chlorophyll variable removed.

Since the MLR model precludes comparison of predicted iron concentrations with, for example, trends in chlorophyll because chlorophyll is included as a variable, we also demonstrated that the MLR approach could be utilized by removing a variable, with some reduction in goodness of fit (Table 2).

3.4. Año Nuevo and Point Sur

[21] Previous research [Bruland *et al.*, 2001; Chase *et al.*, 2005] found that iron values are consistently higher in the Año Nuevo region north of Monterey Bay compared to the Point Sur region south of Monterey Bay (Point Sur; see Figure 1). We therefore examined MODIS optical data for the two regions, summarized in Figure 6. For each year (2002–2007), average b_{bp}/FLH at Año Nuevo was significantly higher than at Point Sur (p value = 0.001, paired t test), supporting the use of this proxy for characterization of broad spatial patterns of labile particulate iron. The seasonal divisions, Upwelling, Oceanic, and Davidson, showed a clear annual pattern at Año Nuevo. For all years that MODIS data were available, the Davidson season exhibited the highest values of b_{bp}/FLH , the Upwelling season was intermediate, and the Oceanic season exhibited the lowest values (Figure 7). These data were analyzed using alternate seasonal divisions described by Elrod *et al.* [2008] and Pennington and Chavez [2000], and the pattern observed (highest b_{bp}/FLH values during the winter) was statistically identical. At Point Sur, the pattern was less consistent, but still present (b_{bp}/FLH was maximal in the Upwelling period for 2 of the 5 years evaluated, otherwise maximal in the Davidson period). An additional location along the Big Sur coast (“BS”; Figure 1) was chosen to further examine the seasonal and interannual trend in predicted iron concentrations and is characterized by a narrow continental shelf. In 2003–2005, the annual average

Figure 5. (a) Measured iron data from the MBARI (solid circles) and CIMT (pluses) programs plotted versus the output from the linear regression model. Error bars represent the coefficient of variation estimates for the in situ iron measurements. (b) The data replotted as quantile-quantile plots with error histograms (inset shows observed minus predicted values for CIMT, dashed line, and MBARI, solid line). The model overpredicts (underpredicts) iron data for MBARI (CIMT) at low concentrations, overpredicts CIMT data at moderate iron concentrations, and slightly underpredicts MBARI data at high concentrations. (c) The same data presented without log-transformation, with the lowest values (0–20 nM iron) included as an inset.



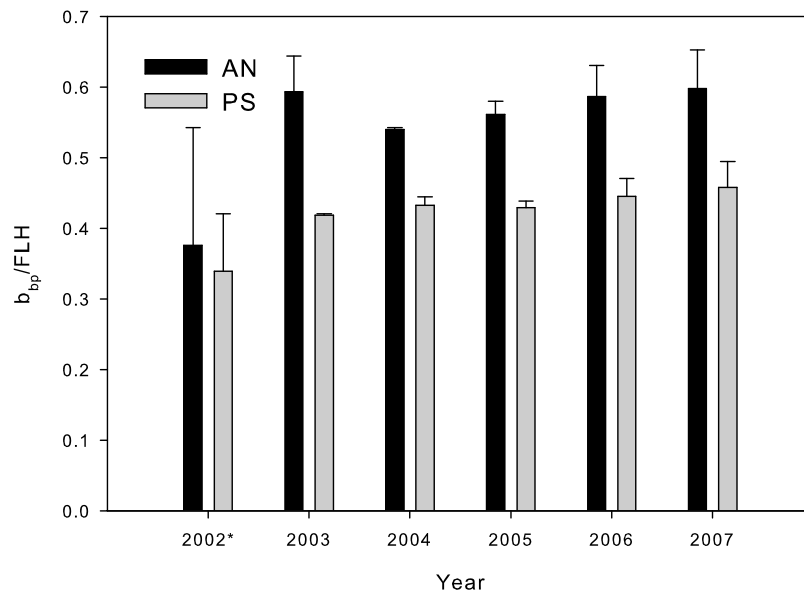


Figure 6. Bars showing b_{bp}/FLH from Año Nuevo (AN) and Point Sur (PS) locations, 2002–2007. Error bars represent the standard deviation of the annual averages.

b_{bp}/FLH at this location was significantly lower than at Año Nuevo. When these data were divided into seasons, the highest values were obtained during the Oceanic season in contrast to the wider shelf regions to the north.

3.5. Spatial and Temporal Variability

[22] Annual average concentrations of dissolvable iron at C1 were higher in all sampling years compared to dissolvable iron concentrations at M1. This trend is clearly visible in the MODIS data as well (Figure 3). Using the CIMT 2002–2007 data set, a distinct pattern emerges when the stations are clustered into regions. In all sampling years there was more HAcFe in the northern part of Monterey Bay (stations T100,

T101 and T102) than at stations T501, T601, and T702 in the southern part of the bay (Figure 2a). During 2003–2006, when backscatter was measured concurrently with the iron, the northern region of the bay exhibited higher values of backscatter/fluorescence in each sampling year than the southern region (Figure 2b). Coupled with the MODIS satellite data for the C1 and M1 locations, the CIMT bio-optical data supports known trends in iron spatial variability in Monterey Bay.

[23] For comparison of predicted labile particulate iron concentrations with previous field efforts, we focus on the Point Sur location used by *Chase et al.* [2005] and a second location along the Big Sur coast, offshore from Point Lopez,

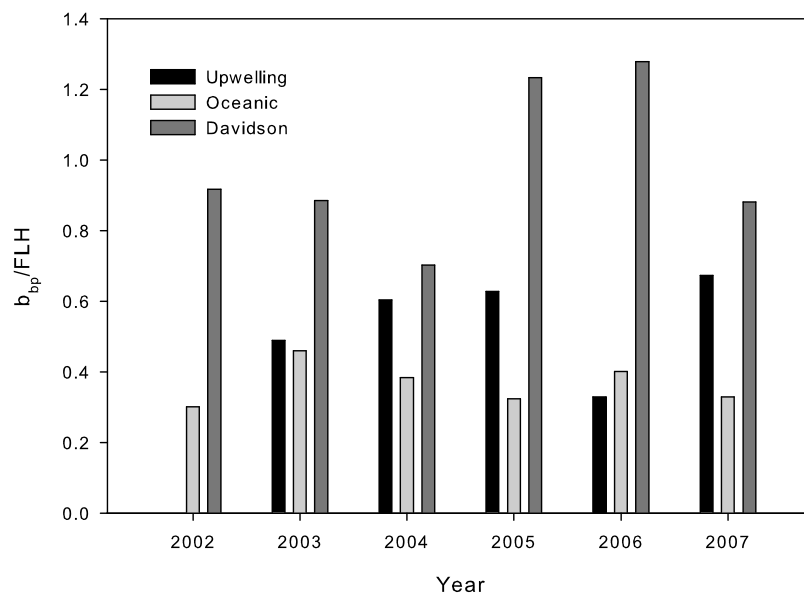


Figure 7. Seasonal averages of b_{bp}/FLH at Año Nuevo. Upwelling is March–June, Oceanic is July–October, and Davidson is November–February.

where *Bruland et al.* [2001] reported very low iron values. The annual averaged MODIS data are lower at Point Sur compared to Año Nuevo. However, when averaged seasonally, an unexpected pattern emerged. In each of the complete data years (MODIS Aqua data are not available prior to July 2002), the highest b_{bp}/FLH occurred during the Oceanic period. In all other locations used for this study, and all years, the Oceanic period exhibited the lowest b_{bp}/FLH , and the lowest directly measured iron concentrations.

[24] Temporally, the optical data at C1 showed the same pattern as DVBLFe, with the highest values during the winter in 2002–2005, and the lowest values during the summer [*Elrod et al.*, 2008]. The optical data at M1 agreed with the measured iron values in 2003, but in 2002, 2004, and 2005 the highest b_{bp}/FLH values occurred in the winter while the highest measured dissolvable iron was in the spring [*Elrod et al.*, 2008]. Unlike central Monterey Bay, there is no comprehensive time series of iron measurements at Año Nuevo or Point Sur. However, a trend exists within the MODIS optical data that suggests an annual pattern of iron in these regions as well. At Año Nuevo the Davidson season exhibited significantly higher b_{bp}/FLH values than the Upwelling or Oceanic periods. The Upwelling period exhibited the second highest b_{bp}/FLH averages, followed by the Oceanic season. At Point Sur, the pattern is less clear. In three of the five years, the Davidson season had the highest b_{bp}/FLH values with the remaining two years maximal during the Upwelling season. Further offshore at Big Sur, the Oceanic season was consistently the highest.

[25] Interannual trends were assessed for C1 and M1 by applying the MBARI MLR model without chlorophyll to monthly data from July 2002 to December 2007, and compared to monthly MODIS chlorophyll for the same period. Trends were analyzed using Sen's slope estimator with a one-tailed Mann-Kendall Tau test. As reported previously [*Kahru et al.*, 2009], there was a significant ($p < 0.05$) increase in chlorophyll, with a trend of 0.092 and 0.068 mg Chl a $m^{-3} y^{-1}$ for C1 and M1. There was no significant increase in MLR-predicted DVBLFe; trend analysis for b_{bp}/FLH was also not significant.

4. Discussion

[26] As coastal regions often experience spatial and temporal variability in iron, there is a need to develop inexpensive, easily accessible methods by which to measure and monitor iron synoptically. Several iron constituents are commonly measured employing a wide variety of methods for trace metal analysis and a correspondingly wide variety of method-specific definitions (e.g., "particulate iron). In Monterey Bay, both CIMT and MBARI measured iron at a similar location for several overlapping years. Several times during the three years when sampling overlapped, data were collected from station T401 (CIMT) and M1 (MBARI) on the same day. However, the two overlapping time series cannot be merged into a longer record, because the two labs were analyzing fundamentally different constituents of the iron pool. The MBARI time series at M1 measured dissolved and dissolvable iron, with dissolvable being unfiltered and acidified to pH 3 [*Elrod et al.*, 2008]. At T401, samples were analyzed for dissolved and acid leachable iron. Processed with a 25% acetic acid leach, this fraction of the total iron is considered

labile and available to phytoplankton [*Bruland et al.*, 2001]. Though the overall trends in iron agree between the two data sets, with annual averaged iron being higher in 2003 and 2005 than in 2004, on a monthly or seasonal scale the two data sets are not comparable, and a paired t test for matching data points from these two labs show only weak correspondence (p value = 0.078). These differences are likely due to both the difference in analytical measurements and the inherent spatial and temporal variability of iron in surface waters.

[27] While iron is difficult and time consuming to measure, many other parameters such as temperature and nutrients that are critical to phytoplankton are more tractable. The primary method for iron delivery to surface waters in Monterey Bay is via the upwelling of cold, saline, and nutrient-rich water to the surface [*Elrod et al.*, 2008; *Fitzwater et al.*, 2003; *Johnson et al.*, 1999]. It is conceivable that a simple proxy could exist for iron concentrations, as elevated iron concentrations are often coupled with high nutrients and low temperatures associated with upwelling. However, past studies have shown that while upwelled water has a characteristic signature that can include high iron, iron is not always associated with freshly upwelled water [*Elrod et al.*, 2008; *Kudela et al.*, 2006]. In Monterey Bay, the first upwelling event of the year brings a large pulse of iron to the surface but subsequent events do not [*Elrod et al.*, 2008; *Johnson et al.*, 2001]. Our results indicate that while during active, early season upwelling elevated iron may correlate with more saline waters, low temperature, and high nitrate, over longer time scales none of these parameters can be used to consistently estimate iron concentrations.

[28] We demonstrate that bio-optical data measured by satellite can be used to determine mesoscale trends in iron concentrations in the coastal ocean, consistent with and complementary to the smaller (San Francisco Bay) and larger (basin scale) assessments using optical data conducted by *Benoit et al.* [2010] and *Behrenfeld et al.* [2009]. Inherent optical properties of the water column can be obtained from satellite observations, either directly or by use of inversion models such as QAA [*Lee et al.*, 2002, 2005]. Fluorescence Line Height is a remotely sensed measurement of solar-induced phytoplankton chlorophyll fluorescence emission spectra, and is often used as a proxy for chlorophyll [*Hoge et al.*, 1999; *Hu et al.*, 2005; *Ryan et al.*, 2009]. FLH can provide more accurate biomass estimates than traditional spectral ratio algorithms for chlorophyll, successfully allowing fluorescence to be distinguished from other optical signatures in surface waters [*Ahn and Shanmugan*, 2007]. For our proxy, FLH is also statistically independent from backscatter using the QAA model, as the FLH wavelengths are not used in the QAA inversion. Thus despite the empirical nature of our derived labile iron proxy, it incorporates information directly linked to fundamental properties of coastal suspended particulate matter.

[29] The bio-optical proxy is further extended using a statistical approach to link readily available environmental parameters to labile particulate iron concentrations. Since the optical properties of the water column are heavily influenced by particle load, one can assume that the physical events carrying iron and other particles to the surface may have a distinct backscatter signature. Several studies in recent years have shown that the bulk refractive index of suspended

particles in seawater can be determined using backscatter and total scatter. Once the bulk refractive index is calculated, the optically dominant particle type can be partitioned into organic or inorganic constituents. It may also be possible to distinguish between different inorganic mineral classes [Boss *et al.*, 2004; Twardowski *et al.*, 2001]. While backscatter may allow identification of inorganic mineral classes present in seawater, fluorescence provides information about living cells. Our approach is entirely empirical, but we suggest that the relationship between optics and iron is based on fundamental properties of surface coastal waters. Backscatter is directly related to particle size, type, and load, while FLH provides information about the relative proportion of living versus detrital or inorganic material, and the relative “health” of the plankton community [cf. Behrenfeld *et al.*, 2009; Kudela *et al.*, 2006].

[30] Our most robust model based on AIC criteria included log-transformed b_{bp}/FLH , log-transformed chlorophyll, sea surface temperature (SST), Pajaro River gage data, and a localized upwelling index calculated for the M1 mooring. Variables considered but discarded included day length (a proxy for seasonality), Salinas River gage data (covarying with the Pajaro River), and the PFEL upwelling index (covarying with the localized index but not statistically significant), all of which can be obtained remotely. While a statistical model does not provide any inherent basis or understanding for why the relationship provides the best fit, we suggest that the positive loadings for river flow and upwelling index provide indications of the source of the particulate material [see also Elrod *et al.*, 2008], the negative loading of SST results from the positive relationship between iron and freshly upwelled (cold) water, while b_{bp}/FLH and chlorophyll are proxies for the composition of the particles and the ecophysiological response to iron availability.

4.1. Spatial and Temporal Patterns

[31] The spatial variations in labile particulate iron concentrations determined using satellite optical data in this study lend support to patterns of iron availability found in previous experiments. Several studies have shown that iron concentrations in surface waters are closely related to the width of the continental shelf in upwelling regions [Bruland *et al.*, 2001; Chase *et al.*, 2005; Hurst and Bruland, 2008; Kudela *et al.*, 2006]. The continental shelf in the Año Nuevo region, situated north of Monterey Bay, varies in width from 20 to 50 km. In contrast, the shelf width along the Big Sur coast in the vicinity of Point Sur is only a few kilometers. Iron concentrations at Año Nuevo are typically greater than those measured at Point Sur, both during active upwelling and before the onset of active upwelling [Bruland *et al.*, 2001; Chase *et al.*, 2005]. The positive relationship between shelf width and predicted iron is also apparent in climatological maps of predicted labile particulate iron (Figure 10).

[32] We observed an unusual seasonal pattern in the Big Sur region, wherein maximal b_{bp}/FLH occurred during the Oceanic period. Without a time series data set available for this region, it is difficult to explain our observed pattern in b_{bp}/FLH . As the shelf is extremely narrow in this region, open ocean conditions exist relatively close to shore. In a noncoastal environment both backscatter and fluorescence measurements are low, which results in a high b_{bp}/FLH ratio, leading to predicted high iron concentrations; our

statistical model accounts for this to some extent with the inclusion of chlorophyll, but it is still likely that the model performs less well in oceanic waters where particulate iron is low to undetectable. MODIS data extracted from locations closer to shore are also influenced by interference from land due to mixed pixel and adjacency effects. In a region of such narrow shelf width, it may not be possible to collect accurate optical backscatter and fluorescence data from satellite measurements that correctly represent conditions on the shelf. It is also important to note that we do not account for changes in phytoplankton species composition. Monterey Bay generally exhibits low total chlorophyll dominated by picoplankton during the Oceanic period [Kudela and Dugdale, 2000; Pennington and Chavez, 2000]. These populations are both less susceptible to iron limitation [Bruland *et al.*, 2001] and exhibit relatively less backscatter compared to larger diatoms and dinoflagellates [Vaillancourt *et al.*, 2004]. Quench-corrected fluorescence has been directly related to iron availability globally [Behrenfeld *et al.*, 2009] with lower fluorescence (FLH) correlated to increasing iron stress. During the Oceanic period we might therefore expect to see changes in both FLH (physiological status) and backscatter driven by shifts in community structure that shift optical properties of the coastal ocean closer to typical open ocean conditions. We do not take these factors into account, potentially leading to discrepancies, particularly during oceanic conditions. Alternatively, the patterns derived from MODIS may be accurate, but the lack of long-term in situ data sets to compare with for this region makes this impossible to validate.

[33] Iron values consistently show an onshore to offshore gradient of decreasing concentration in the Monterey Bay region [Johnson *et al.*, 2001]. C1 is located on the continental shelf at the head of the Monterey Canyon with a water depth of 230 m, and M1 is located over the canyon in 1200 m water depth [Johnson *et al.*, 2001]. The northern CIMT stations are also located over a broad expanse of shelf in a region that has several river mouths, which may account for the higher iron values recorded by the CIMT program. T100 and T101 are also located within the path of the plume of upwelled water that extends southward from the Davenport region during the upwelling season [Pennington and Chavez, 2000]. This plume transports cold, saline water across Monterey Bay, and could possibly transport iron from the shelf near Davenport [Fitzwater *et al.*, 2003].

[34] One possible reason for the discrepancy between the temporal patterns exhibited from the in situ DVBLFe and our proxy data (Figure 8) is the lack of iron measurements during winter storms. During the winters of 2002, 2003, and 2004, there were no in situ iron measurements taken for periods of 51, 38, and 64 days, respectively [Elrod *et al.*, 2008]. Johnson *et al.* [2001], using the same iron data set from the M1 and C1 moorings as used here, described seasonality of dissolvable iron for Monterey Bay. They determined that iron concentrations peak with the onset of spring upwelling, and then diminish, though upwelling continues [Johnson *et al.*, 2001]. Bio-optical measurements support annual patterns of high and low iron concentrations. Data from MODIS show similar monthly trends as the in situ iron measured at C1, with a peak in b_{bp}/FLH that corresponds to each recorded high-iron event (Figure 8). Although there are peaks in the optical data that do not correspond with

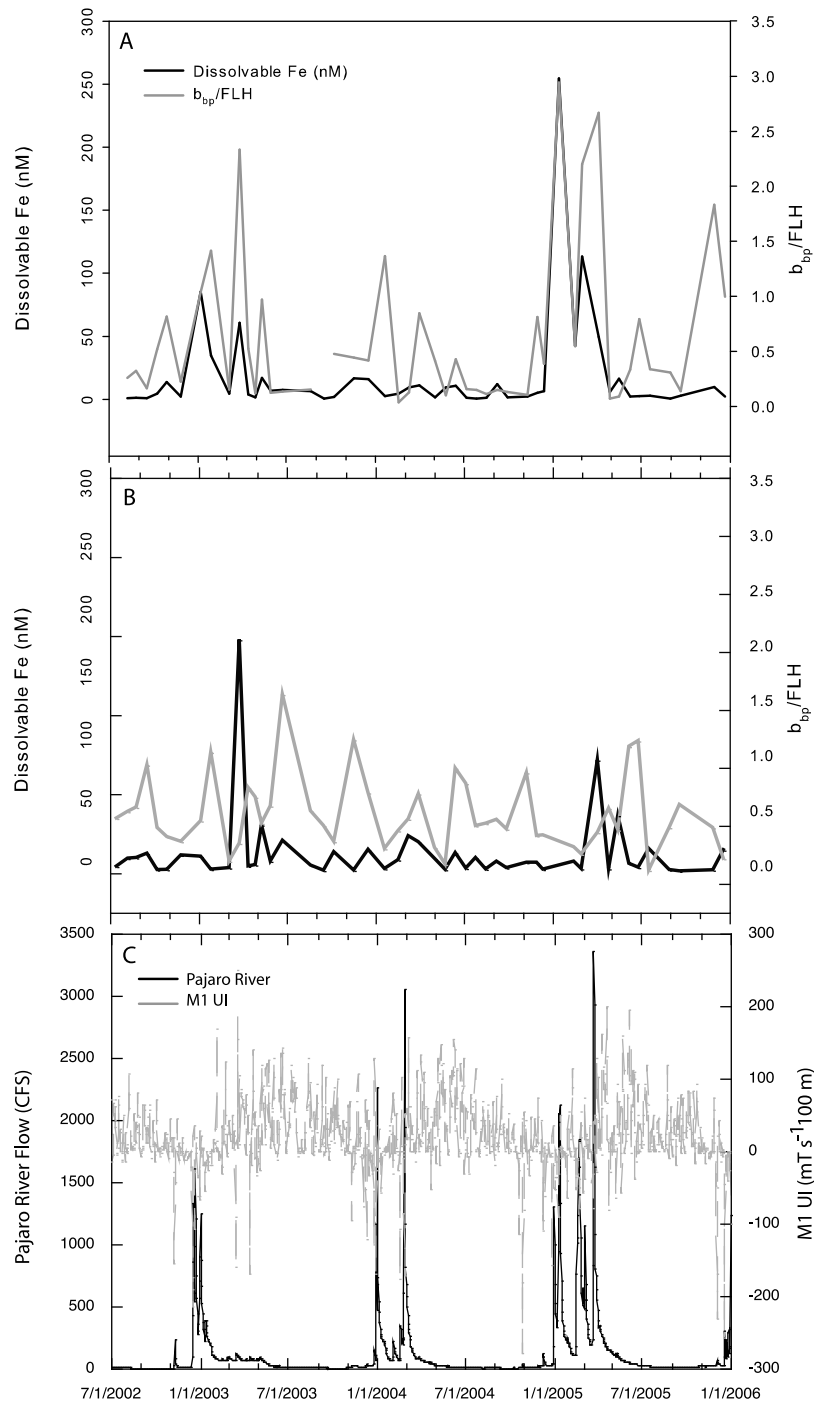


Figure 8. (a) The b_{bp}/FLH and dissolvable iron (nM) through time at C1, 2002–2005. (b) The same for station C2. (c) The M1 upwelling index and Pajaro River flow data for the same time period at 1 day resolution.

high-iron events, this could easily be a result of missing in situ data due to shipboard sampling limitations.

4.2. Biological Response

[35] When considering the relationship between iron and chlorophyll in Monterey Bay, some interesting patterns emerged from the data. *Elrod et al.* [2008] reported that during the summer months (June–October), chlorophyll and dissolvable iron are highly correlated for the MBARI M1

and M2 mooring locations. At M1, the summer months showed a slightly better correlation ($R^2 = 0.362$) than the rest of the year, but chlorophyll at this location was not well correlated with dissolvable iron. The data presented by *Elrod et al.* [2008] included the summer months at the M2 mooring, which is located ~ 45 km from shore. As iron values were shown in that work to be considerably lower at M2 than M1, it is likely that chlorophyll and iron are much more closely coupled at the M2 mooring. We suggest that the large

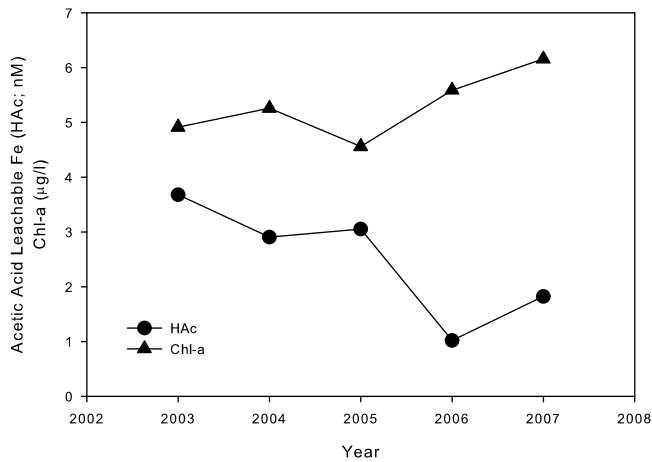


Figure 9. Annual averages of HAcFe (nM) and total chlorophyll *a* ($\mu\text{g/L}$), all CIMT stations combined, 2003–2007.

dynamic range in chlorophyll and iron presented by *Elrod et al.* [2008] may result in a more robust iron:chlorophyll relationship, similar to the much better optical:iron relationship seen off the northern California coast where there was an order of magnitude greater signal as described by *Kudela et al.* [2006].

[36] Iron and chlorophyll data from the CIMT stations also showed a lack of correlation, but also exclude the offshore (oceanic) waters included in the *Elrod et al.* [2008] study. Between 2003 and 2007 the years with the highest average annual iron (2003 and 2005) also had the lowest average total chlorophyll. The years with the highest average chlorophyll (2006 and 2007) had the lowest iron (Figure 9). Though there is some degree of seasonal correlation, when considering an entire year chlorophyll and iron are clearly uncoupled in the highly productive nearshore waters. Similar analysis of the size-fractionated chlorophyll versus iron (not shown) demonstrate no significant patterns in phytoplankton size structure, despite the observations reported by *Johnson et al.* [1999] suggesting a seasonal progression from large cells (diatoms) to smaller cells as dissolvable iron was depleted in surface waters. This annual trend of high chlorophyll and low iron, and lack of a seasonal trend in phytoplankton size structure versus iron, suggests that nearshore phytoplankton populations may at times be more heavily controlled by top-down factors, or, alternatively, non-correlating bottom-up factors, than by iron availability. This is supported at interannual time scales by the satellite-derived observation of increasing chlorophyll in Monterey, similar to the trends reported for Southern California by *Kim et al.* [2009] and for Monterey Bay using in situ data (available from the Monterey Bay Aquarium Research Institute, <http://www.mbari.org/bog/mb/Trends.htm>). There was no corresponding trend in either the bio-optical proxy or the MLR model, suggesting that these multiyear increases in phytoplankton biomass are not directly associated with changes in dissolvable iron, and further suggesting (as noted by *Elrod et al.* [2008]) that iron limitation is not typically evident in the nearshore waters (inshore of M2) of Monterey Bay.

[37] There appears to be little relationship between iron availability and “wet” and “dry” years despite the general correspondence between periods of river flow and iron

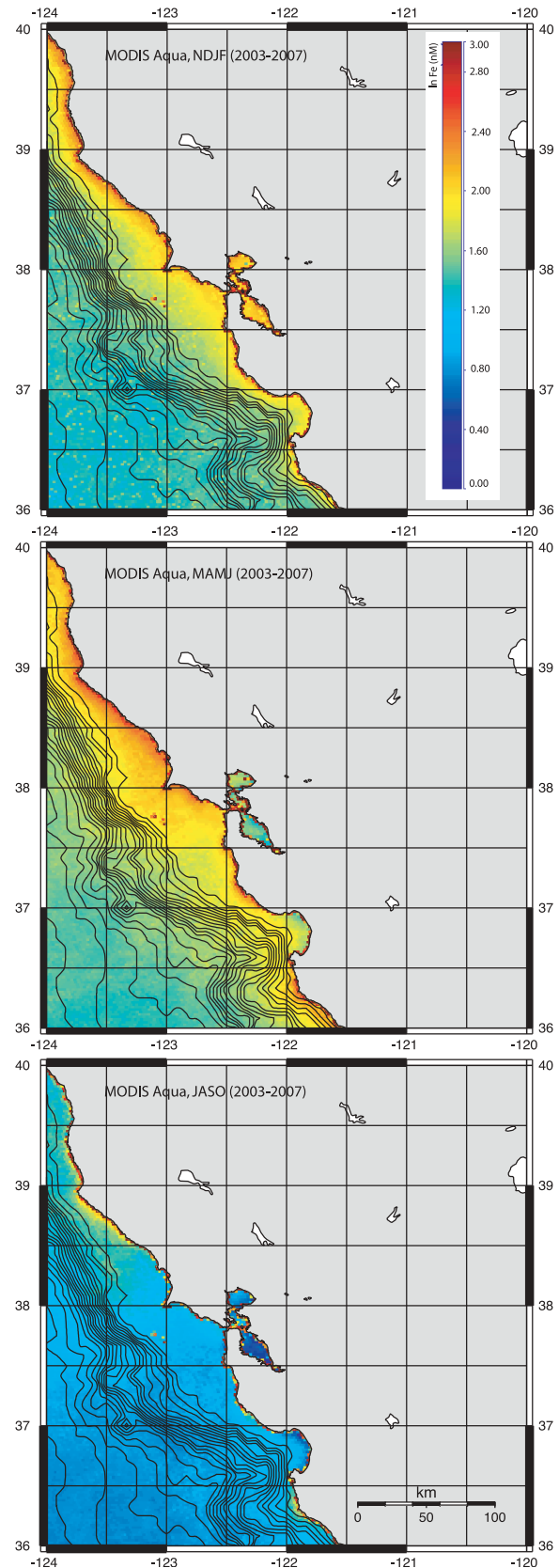


Figure 10. Seasonal spatial maps of log-transformed predicted labile particulate iron concentrations, 2003–2007. Values are calculated using equation (1) with data sources listed in Table 1.

(Table 1 and Figure 8). Despite the relatively strong partial correlation between river flow and iron estimates, the model weighting was low (Table 1), and there was no significant correlation between annual-averaged iron estimates (from any data set) and annual-averaged river flow. This is consistent with the work of Chase *et al.* [2007], who argued that the Oregon shelf acts as an iron “capacitor” buffering the biological response from the seasonal and interannual variability of iron inputs, resulting in no direct correlation between river flow and chlorophyll [Chase *et al.*, 2007] or particulate iron (our data).

4.3. Applications for the Bio-optical Iron Proxy

[38] Direct comparison of the remotely sensed bio-optical proxy and the subsequently developed statistical model for iron versus measured HAcFe and DVBLFe lend support to the use of b_{bp}/FLH as a proxy for labile particulate iron in surface coastal waters. In order to expand our investigation of the proxy to a larger area, we created spatial maps of b_{bp}/FLH for Monterey Bay and the surrounding coastal region (Figure 10). We used five years of MODIS Aqua data (2003–2007) temporally averaged into climatological Upwelling, Oceanic, and Davidson seasons in conjunction with the ancillary data and the statistical model presented in Table 1. There are higher levels of predicted iron where the continental shelf is relatively wide, near Año Nuevo, and lower levels along the Big Sur Coast. Additionally, the Oceanic period shows the lowest levels of predicted iron for the annual cycle, indicative of low levels of iron throughout the region, while Upwelling and Davidson show much greater predicted iron values.

[39] As we have focused this investigation primarily on the central California coast, and Monterey Bay in particular, further research is necessary before this proxy can be applied to other coastal regimes, and there are likely limitations in applying this proxy very far beyond the continental shelf [see also Kudela *et al.*, 2006]. Satellite or in situ optical data should be applied in conjunction with iron measurements in order to test the utility of this proxy in other regions; however, the statistically robust relationships we report here are likely applicable to similar regimes within the California Current, and possibly to other upwelling systems that exhibit spatial and temporal fluctuations in labile particulate iron (e.g., Peru [Bruland *et al.*, 2005]). A caveat of our models is the tradeoff between using a purely optical proxy (b_{bp}/FLH) and a statistical model incorporating other environmental variables. For example, it is not possible to examine the relationship between labile particulate iron and river flow if both variables are included in the predictive model. While b_{bp}/FLH could be used directly, there is a substantial decrease in accuracy compared to the full statistical model(s). The inclusion of region-specific parameters would also need to be assessed for each region where a bio-optical iron proxy (outside of Monterey Bay) was applied.

5. Summary

[40] Ten years of data collected in Monterey Bay by MBARI and CIMT, as well as data accessed from the MODIS Aqua satellite, clearly indicate that bio-optical measurements can be used as a proxy to estimate patterns of labile particulate iron. This optical proxy is statistically

robust but weakly correlated with observations from two commonly used, but distinct, methods for estimating in situ iron concentrations. On the basis of previous studies, we assume that these particulate iron measurements are a good proxy for the “bio-available” iron pool. Using the ratio of backscatter and fluorescence collected through commercially available optical instrumentation, or the ratio of backscatter and fluorescence line height collected by the MODIS Aqua sensor, broad patterns of surface iron concentrations can be determined. Incorporating other environmental variables via regression models can further improve the estimates for regional assessments, albeit at the risk of conflating iron estimates with other variables of interest. Though neither this proxy nor the MLR models will replace standard methods for measuring in situ iron concentrations, these methods can be a valuable tool to oceanographers working in coastal regions. Using an optical method for particulate iron estimates allows patterns of surface iron concentrations to be remotely determined over broad expanses of space and time. So long as MODIS or a comparable satellite is available, our method can also be extended indefinitely into the future. While 5+ years of data are not sufficient for examining long-term interannual trends, the potential exists for such an analysis in the next few years.

[41] **Acknowledgments.** We thank Ken Bruland and Ken Johnson and their lab groups for access to the iron data, in particular, Virginia Elrod from the Johnson Lab and Sherry Lippiatt from the Bruland Lab; we also thank Jenny Quay for providing the upwelling index and river flow data and for critical comments, the captain and crew of the R/V *John Martin*, and the other CIMT participants. This manuscript was substantially improved by comments from three anonymous reviewers. This work was partially supported by NOAA through the Center for Integrated Marine Technology, award NA160C2936 (R.M.K.), the National Science Foundation grant OCE-726858 (R.M.K.), the National Aeronautics and Space Administration grant NNX09AT01G (R.M.K.), and the Center for Remote Sensing at UCSC (A.R.M.).

References

- Ahn, Y., and P. Shanmugan (2007), Derivation and analysis of the fluorescence algorithms to estimate phytoplankton pigment concentrations in optically complex coastal waters, *J. Opt. A Pure Appl. Opt.*, *9*, 352–362, doi:10.1088/1464-4258/9/4/008.
- Behrenfeld, M. J., et al. (2009), Satellite-detected fluorescence reveals global physiology of ocean phytoplankton, *Biogeosciences*, *6*, 779–794, doi:10.5194/bg-6-779-2009.
- Benoit, M. D., R. M. Kudela, and A. R. Flegal (2010), Modeled trace element concentrations and partitioning in the San Francisco estuary, based on suspended solids concentration, *Environ. Sci. Technol.*, *44*, 5956–5963, doi:10.1021/es1001874.
- Boss, E., W. S. Pegau, M. Lee, M. Twardowski, E. Shybanov, G. Korotaev, and F. Baratange (2004), Particulate backscattering ratio at LEO 15 and its use to study particle composition and distribution, *J. Geophys. Res.*, *109*, C01014, doi:10.1029/2002JC001514.
- Boyd, P., et al. (2007), Mesoscale iron enrichment experiments 1993–2005: Synthesis and future directions, *Science*, *315*, 612–617, doi:10.1126/science.1131669.
- Bruland, K. W., E. L. Rue, and G. J. Smith (2001), Iron and macronutrients in California coastal upwelling regimes: Implications for diatom blooms, *Limnol. Oceanogr.*, *46*(7), 1661–1674, doi:10.4319/lo.2001.46.7.1661.
- Bruland, K. W., E. L. Rue, G. J. Smith, and G. R. DiTullio (2005), Iron, macronutrients and diatom blooms in the Peru upwelling regime: Brown and blue waters of Peru, *Mar. Chem.*, *93*, 81–103, doi:10.1016/j.marchem.2004.06.011.
- Buck, K. R., M. C. Lohan, C. J. M. Berger, and K. W. Bruland (2007), Dissolved iron speciation in two distinct river plumes and an estuary: Implications for riverine iron supply, *Limnol. Oceanogr.*, *52*(2), 843–855, doi:10.4319/lo.2007.52.2.0843.
- Chase, Z., B. Hales, T. Cowles, R. Schwartz, and A. van Geen (2005), Distribution and variability of iron input to Oregon coastal waters during the

- upwelling season, *J. Geophys. Res.*, *110*, C10S12, doi:10.1029/2004JC002590.
- Chase, Z., P. G. Stratton, and B. Hales (2007), Iron links river runoff and shelf width to phytoplankton biomass along the U.S. West Coast, *Geophys. Res. Lett.*, *34*, L04607, doi:10.1029/2006GL028069.
- Elrod, V. A., K. S. Johnson, S. E. Fitzwater, and J. Plant (2008), A long-term, high-resolution record of surface water iron concentrations in the upwelling-driven central California region, *J. Geophys. Res.*, *113*, C11021, doi:10.1029/2007JC004610.
- Fitzwater, S. E., K. S. Johnson, V. A. Elrod, J. P. Ryan, L. J. Coletti, S. J. Tanner, R. M. Gordon, and F. P. Chavez (2003), Iron, nutrient and phytoplankton biomass relationships in upwelled waters of the California coastal system, *Cont. Shelf Res.*, *23*, 1523–1544, doi:10.1016/j.csr.2003.08.004.
- Hoge, F., C. Wright, P. Lyon, R. Swift, and J. Yungel (1999), Satellite retrieval of the absorption coefficient of phytoplankton phycoerythrin pigment: Theory and feasibility status, *Appl. Opt.*, *38*(36), 7431–7441, doi:10.1364/AO.38.007431.
- Hu, C., F. E. Muller-Karger, C. J. Taylor, K. L. Carder, C. Kelble, E. Johns, and C. A. Heil (2005), Red tide detection and tracing using MODIS fluorescence data: A regional example in SW Florida coastal waters, *Remote Sens. Environ.*, *97*, 311–321, doi:10.1016/j.rse.2005.05.013.
- Hurst, M. P., and K. W. Bruland (2008), The effects of the San Francisco Bay plume on trace metal and nutrient distributions in the Gulf of the Farallons, *Geochim. Cosmochim. Acta*, *72*, 395–411, doi:10.1016/j.gca.2007.11.005.
- Hutchins, D. A., and K. W. Bruland (1998), Iron-limited diatom growth and Si:N uptake ratios in a coastal upwelling regime, *Nature*, *393*, 561–564, doi:10.1038/31203.
- Hutchins, D., G. DiTullio, Y. Zhang, and K. Bruland (1998), An iron limitation mosaic in the California upwelling regime, *Limnol. Oceanogr.*, *43*(6), 1037–1054, doi:10.4319/lo.1998.43.6.1037.
- Hutchins, D. A., et al. (2002), Phytoplankton iron limitation in the Humboldt Current and Peru Upwelling, *Limnol. Oceanogr.*, *47*(4), 997–1011, doi:10.4319/lo.2002.47.4.0997.
- Johnson, K. S., F. P. Chavez, and G. E. Friederich (1999), Continental shelf sediment as a primary source of iron for coastal phytoplankton, *Nature*, *398*, 697–700, doi:10.1038/19511.
- Johnson, K. S., F. P. Chavez, V. A. Elrod, S. E. Fitzwater, J. T. Pennington, K. R. Buck, and P. M. Walz (2001), The annual cycle of iron and the biological response in central California coastal waters, *Geophys. Res. Lett.*, *28*(7), 1247–1250, doi:10.1029/2000GL012433.
- Johnson, K. S., et al. (2003), Surface ocean-lower atmosphere interactions in the Northeast Pacific Ocean Gyre: Aerosols, iron, and the ecosystem response, *Global Biogeochem. Cycles*, *17*(2), 1063, doi:10.1029/2002GB002004.
- Johnson, K. S., et al. (2007), The SAFe Iron Intercomparison Cruise: An international collaboration to develop dissolved iron in seawater standards, *Eos Trans. AGU*, *88*, 131–132, doi:10.1029/2007EO110003.
- Kahru, M., et al. (2009), Trends in primary production in the California Current detected with satellite data, *J. Geophys. Res.*, *114*, C02004, doi:10.1029/2008JC004979.
- Kim, H.-J., et al. (2009), Coastal phytoplankton blooms in the Southern California Bight, *Prog. Oceanogr.*, *82*, 137–147, doi:10.1016/j.pocan.2009.05.002.
- Kudela, R. M., and R. C. Dugdale (2000), Nutrient regulation of phytoplankton productivity in Monterey Bay, California, *Deep Sea Res., Part II*, *47*, 1023–1053, doi:10.1016/S0967-0645(99)00135-6.
- Kudela, R. M., N. Garfield, and K. W. Bruland (2006), Bio-optical signatures and biogeochemistry from intense upwelling and relaxation in coastal California, *Deep Sea Res., Part II*, *53*, 2999–3022, doi:10.1016/j.dsr2.2006.07.010.
- Landing, W. M., and K. W. Bruland (1987), The contrasting biogeochemistry of iron and manganese in the Pacific Ocean, *Geochim. Cosmochim. Acta*, *51*, 29–43, doi:10.1016/0016-7037(87)90004-4.
- Lee, Z. P., K. L. Carder, and R. Arnone (2002), Deriving inherent optical properties from water color: A multi-band quasi-analytical algorithm for optically deep waters, *Appl. Opt.*, *41*, 5755–5772, doi:10.1364/AO.41.005755.
- Lee, Z. P., M. Darecki, K. L. Carder, C. O. Davis, D. Stramski, and W. J. Rhea (2005), Diffuse attenuation coefficient of downwelling irradiance: An evaluation of remote sensing methods, *J. Geophys. Res.*, *110*, C02017, doi:10.1029/2004JC002573.
- Nezlin, N. P., P. G. DiGiacomo, D. W. Diehl, B. H. Jones, S. C. Johnson, M. J. Mengel, K. M. Reifel, J. A. Warrick, and M. Wang (2008), Stormwater plume detection by MODIS imagery in the Southern California coastal ocean, *Estuarine Coastal Shelf Sci.*, *80*, 141–152, doi:10.1016/j.ecss.2008.07.012.
- Obata, H., H. Karatani, and E. Nakayama (1993), Automated determination of iron in seawater by chelating resin concentration and chemiluminescence detection, *Anal. Chem.*, *65*, 1524–1528, doi:10.1021/ac00059a007.
- Palacios, S. L., T. D. Peterson, and R. M. Kudela (2009), Development of synthetic salinity from remote sensing for the Columbia River plume, *J. Geophys. Res.*, *114*, C00B05, doi:10.1029/2008JC004895.
- Pennington, J. T., and F. P. Chavez (2000), Seasonal fluctuations of temperature, salinity, nitrate, chlorophyll, and primary production at station H3/M1 over 1989–1996 in Monterey Bay, California, *Deep Sea Res., Part II*, *47*, 947–973, doi:10.1016/S0967-0645(99)00132-0.
- Rue, E. L., and K. W. Bruland (2001), Domoic acid binds iron and copper: A possible role for the toxin produced by the marine diatom *Pseudo-nitzschia*, *Mar. Chem.*, *76*, 127–134, doi:10.1016/S0304-4203(01)00053-6.
- Ryan, J. P., A. M. Fischer, R. M. Kudela, J. F. R. Gower, S. A. King, R. Marin III, and F. P. Chavez (2009), Influences of upwelling and downwelling winds on red tide bloom dynamics in Monterey Bay, California, *Cont. Shelf Res.*, *29*, 785–795, doi:10.1016/j.csr.2008.11.006.
- Skogsberg, T., and A. Phelps (1946), Hydrography of Monterey Bay, California: Thermal conditions, Part II, 1934–1937, *Proc. Am. Philos. Soc.*, *90*, 350–386.
- Twardowski, M. S., E. Boss, J. B. Macdonald, W. S. Pegau, A. H. Bernard, and J. R. V. Zaneveld (2001), A model for estimating bulk refractive index from the optical backscattering ratio and the implications for understanding particle composition in case I and case II waters, *J. Geophys. Res.*, *106*, 14,129–14,142, doi:10.1029/2000JC000404.
- Vaillancourt, R. D., C. W. Brown, R. R. L. Guillard, and W. M. Balch (2004), Light backscattering properties of marine phytoplankton: Relationship to cell size, chemical composition and taxonomy, *J. Plankton Res.*, *26*, 191–212, doi:10.1093/plankt/fbh012.
- Ware, D. M., and R. E. Thomson (2005), Bottom-up ecosystem trophic dynamics determine fish production in the Northeast Pacific, *Science*, *308*, 1280–1284, doi:10.1126/science.1109049.
- Warrick, J. A., P. M. DiGiacomo, S. B. Weisberg, N. P. Nezlin, M. Mengel, B. H. Jones, J. C. Ohmann, L. Washburn, E. J. Terrill, and K. L. Farnsworth (2007), River plume patterns and dynamics within the Southern California Bight, *Cont. Shelf Res.*, *27*, 2427–2448, doi:10.1016/j.csr.2007.06.015.
- Wells, M. L., C. G. Trick, W. P. Cochlan, M. P. Hughes, and V. L. Trainer (2005), Domoic acid: The synergy of iron, copper, and the toxicity of diatoms, *Limnol. Oceanogr.*, *50*(6), 1908–1917, doi:10.4319/lo.2005.50.6.1908.
- Welschmeyer, N. A. (1994), Fluorometric analysis of Chlorophyll a in the presence of Chlorophyll b and pheopigments, *Limnol. Oceanogr.*, *39*(8), 1985–1992, doi:10.4319/lo.1994.39.8.1985.

R. M. Kudela and A. R. McGaraghan, Department of Ocean Sciences, University of California, 1156 High St., Santa Cruz, CA 95064, USA. (kudela@ucsc.edu)